Observations and analytical modeling of freshwater and rainwater lenses in coastal dune systems

Stuyfzand, Pieter J.

Important note
To cite this publication, please use the final published version (if applicable).
Please check the document version above.

Observations and analytical modeling of freshwater and rainwater lenses in coastal dune systems

Pieter J. Stuyfzand[1,2]

Abstract Observations are reported on (i) groundwater recharge rates under various types of vegetation as measured with megalysimeters in the dunes, (ii) freshwater lenses along the Dutch North Sea coast in the early 1900s, and (iii) rainwater lenses that develop on top of laterally migrating, artificially recharged riverwater. Subsequently analytical methods are presented to estimate annual natural groundwater recharge as function of rainfall and vegetation, and to calculate the size, shape and transition zone of freshwater lenses on saline groundwater and rainwater lenses on infiltrated riverwater. An empirical correction factor, based on the hydraulic resistance of an aquitard within the freshwater lens, is proposed to account for the frequently observed reduction of the Ghyben-Herzberg ratio of 40. This factor raises the groundwater table, reduces the depth of the fresh/salt interface and increases the lens formation time. The suite of methods offers a tool box for knowledge based water management of dune systems, by rapidly predicting: (i) more or less autonomous changes due to sealevel rise, climate change and vegetation development; and (ii) the potential (side) effects of interventions. Knowing what happened or will happen to the fresh water lens or a rainwater lens is important, because changes impact on important natural habitat parameters such as salinity, depth to groundwater table, decalcification rate (and thus on pH, Ca/Al, PO_4, NH_4) and nutrient availability, and on

drinking water supply. The analytical models are applied to predict effects of sealevel rise, coastal progradation, vegetation changes, and increased temperature of coastal air and river water to be infiltrated.

Keywords Coastal dunes · Evapotranspiration · Freshwater lens · Artificial recharge · Rainwater lens · Sea level rise · Climate change

Introduction

How to safeguard and manage coastal dune areas, is becoming a very urgent question necessitating international knowledge exchange, multidisciplinary research and action (among others: Van der Meulen et al. 1989; Bakker et al. 1990; Salman and Bonazountas 1996; Herrier et al. 2005; Geelen et al. 2015). The urgency is first of all dictated by a worldwide coastline erosion or retreat due to sealevel rise, land subsidence or human drivers of land loss (Bird 1981; Hansom 2001; IPCC 2007). Narrowing of the dune width will result in a drawdown of the groundwater table and shrinking of the fresh water lens (Bakker 1981; Stuyfzand 1993; Oude Essink 1996), with further consequences for vegetation cover and groundwater abstraction.

Other reasons for urgency are composed of climate change conducing to global heating, locally more rainfall and more frequent droughts and extreme rainfall events (IPCC 2007), intensifying anthropogenic pressures (Curr et al. 2000; Brown and McLachlan 2002; Defeo et al. 2009), a still too high atmospheric deposition of NO_X and NH_Y (Grootjans et al. 2013; Kooijman et al. 1998), and lack of aeolian dynamics (Arens and Geelen 2006; Geelen et al. 2015) with resulting irreversible decalcification and acidification (Grootjans et al. 1997; Stuyfzand 1998).

✉ Pieter J. Stuyfzand
pieter.stuyfzand@kwrwater.nl

[1] KWR Watercycle Research Institute, P.O. Box 1072, 3430 Nieuwegein, BB, Netherlands

[2] Department Geoscience and Engineering, Section Geo-Environmental Engineering, Delft University of Technology, P.O. Box 5048, 2600 Delft, GA, Netherlands

 Springer

In this contribution, the focus is on the genesis, occurrence and analytical modeling of freshwater lenses on saline groundwater and rainwater lenses on infiltrated riverwater. Freshwater lenses are formed by rainfall and infiltration on land with saline water in the underground. They can be very small (few meters diameter, <1 m deep) below embryo dunes on the beach, and very large (100 km long, up to 5 km wide, and up to 140 m deep) along wide dune coasts such as in the Western Netherlands (Stuyfzand 1993). These lenses are extremely important for fresh water supply to among others phreatophytic plant communities, wildlife and man.

Rainwater lenses form where rain is falling and infiltrating on land next to infiltrating water courses such as recharge basins or influent rivers. The term is generally used to denote a thin, shallow layer of nutrient-poor, autochthonous groundwater or acid groundwater similar to rain water, on top of laterally migrating, eutrophic, slightly more mineralized groundwater of fluvial or lacustrine origin. The presence of sufficiently thick rainwater lenses is important for the survival of rare plant species in wet dune valleys adjacent to recharge basins, because phreatophytes like reeds can reach and profit from the more eutrophic, infiltrated surface water below thin lenses and thus overshadow rare plant species (Van Dijk 1989).

Groundwater recharge by rainfall is a very important parameter in modeling both lens types. In this paper, the results of 60 years of monitoring at megalysimeter station Castricum are presented, and used to develop a simple approximation method for annual recharge as function of rainfall and 11 types of vegetation.

Field data of Dutch coastal freshwater lenses in the early 1900s are presented to show details of their accurately measured size, shape and transition zone in relatively undisturbed condition, and to derive a new, closed-form analytical solution to account for the often neglected presence of an aquitard within (!) the freshwater lens, which reduces the Ghyben-Herzberg ratio. Solutions for various idealized hydrogeological settings by among others Verruijt (1971), Fetter (1972), Bakker (1981), Huisman and Olsthoorn (1983), Vacher (1988), Stuyfzand and Bruggeman (1994), Chesnaux and Allen (2008) and Greskowiak et al. (2012) are also presented here, in order to supply a tool box for knowledge based water management of dune systems, by yielding insight into: (i) more or less autonomous changes due to sealevel rise, climate change and vegetation development; and (ii) the potential (side) effects of interventions.

Interventions could consist of for instance the reduction of vegetation density, artificial recharge or coastal progradation by large scale beach or foreshore nourishments. In the Netherlands, coastal defence policy changed in 1990 from defensive to offensive, by applying large scale nourishments using sand from the North Sea floor about 20 km offcoast (Hillen and Roelse 1995; Grunnet et al. 2004; Vidal and Van Oord 2010; Huizer et al. 2016). Also in the Netherlands, salinization and desiccation of its coastal dune aquifers have been largely reversed since the mid 1950s, by large scale artificial recharge using pretreated Rhine and Meuse River waters (Stuyfzand 1993).

Material and methods

Field sites

The field sites are situated in the coastal dune area at the edge of the Rhine delta, in the southeastern marginal part of the North Sea basin (Fig.1), approximately at 4°30' E and 52°30' N. The area is about 350 km long and max. 10 km across, with an altitude of 6 m BSL (Below Sea Level) to 52 m ASL (Above Sea Level).

The climate can be defined as a temperate, rainy, marine climate. The predominant wind blows from the southwest, mean air temperature is about 11 °C and mean annual precipitation amounts to 0.82 m. Geological formations to a depth of 50 m (in the south) and 450 m BSL in the north consist of unconsolidated sediments of Quarternary age, deposited in (peri)marine, aeolian, paludal, fluvial, peri-glacial and even glacial environments (Jelgersma et al. 1970; Zagwijn 1985). Along the coast above 2 to 5 m BSL, the deposits generally consist of dune sand on top of beach and shallow marine sands. Holocene aquitards composed of very fine silty sand, clay or peat, often somewhere between 7 and 20 m BSL, frequently separate the upper phreatic aquifer from the semiconfined second aquifer below (Stuyfzand 1993).

Groundwater abstraction from the phreatic dune aquifer, mainly for drinking water supply, started in 1853 on site 15 (Fig.1), after which other sites followed. Growing water demands stimulated the exploration and exploitation of the semiconfined, deeper aquifer in the early 1900s. In the mid 1950s salinization forced the water supply companies on most of sites 12–21 to apply artificial recharge with pretreated surface waters mainly deriving from the Rhine River and Meuse River (Stuyfzand 1993).

Near Bergen aan Zee (between site 10 and 11 in Fig.1), the so-called calcium carbonate transtion zone separates calcareous dune sand (3.5 % $CaCO_3$) in the south from calcite poor dune sand (0.5–1.0 %) in the north (Eisma 1968; Stuyfzand et al. 2012).

Lysimeters

The 4 M-lysimeters are situated ~1 km to the west of Castricum and 2 km to the east of the North Sea beach, near site 12 (Fig.1). They belong to the drainage type (not weighable) and form together the largest lysimeter combination in the world (each lysimeter being 25 × 25 m and 2.5 m deep). They are also unique regarding their hydrological setting,

Fig. 1 Location map showing the 21 coastal dune areas along the Dutch North Sea coast listed in Table 3, with details of lysimeter station Castricum. Background map of Netherlands with Holocene deposits according to Berendsen and Stouthamer 2001
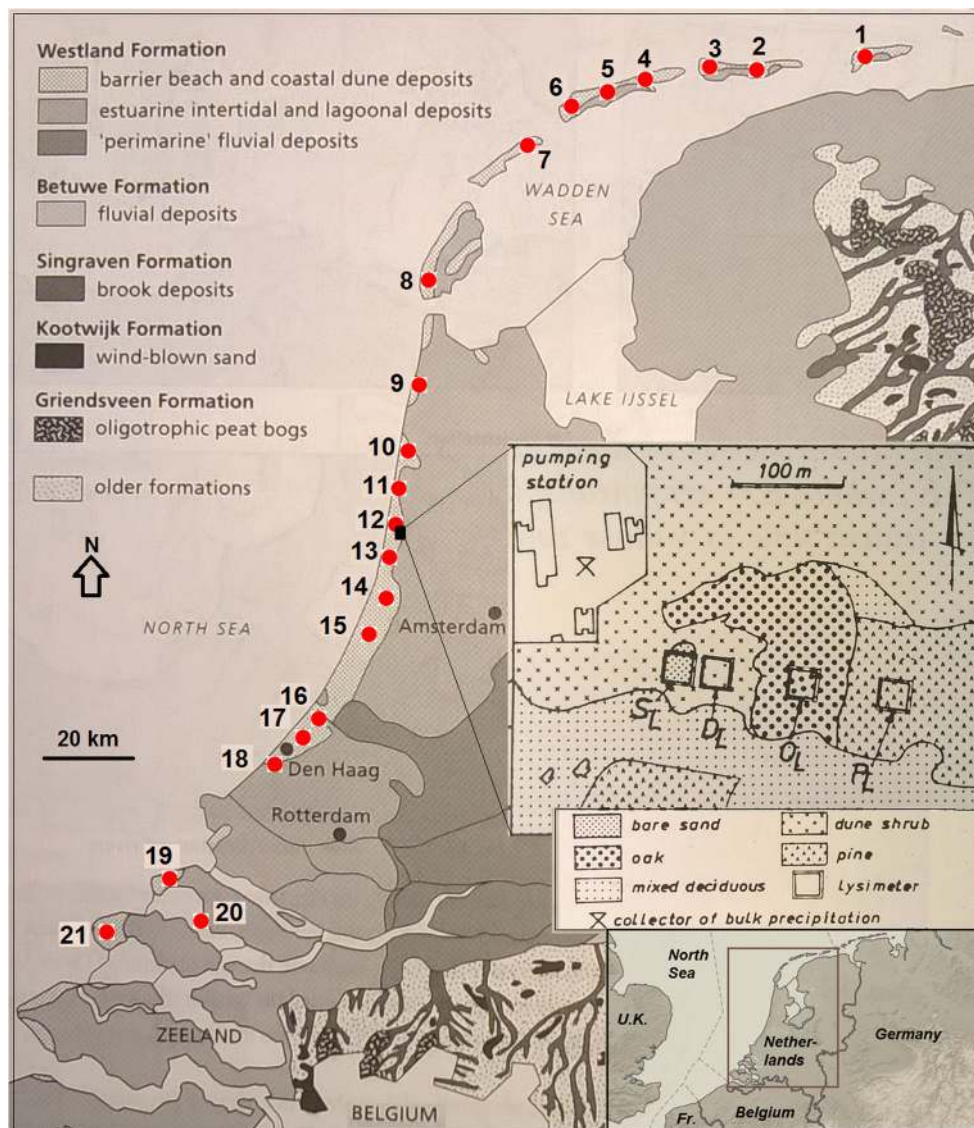
because they are located in calcareous coastal dunes with the following set of natural vegetation types: bare sand (lys.1), dune shrub (lys.2), oaks (lys.3) and pines (lys.4).

Groundwater observations

In the early 1900s exploratory wells for the deeper fresh groundwater reserves in the coastal dune areas often applied temporary, 1 m long well screens which were installed and subsequently withdrawn during bailer drilling of monitor wells up to 350 m deep. This yielded very detailed, vertical hydraulic and hydrochemical logs of the fresh water lens in relatively little disturbed conditions prior to large scale extraction for drinking water supply (Stuyfzand 1993). Monitoring wells were and still are constructed by installing several (mostly 5–10) piezometers of 1–2 m length in one borehole often 80–150 m deep, with clay plugs in between and where aquitards are pierced. A unique number of

observation wells accrued thanks to (i) needs for exploration, monitoring of salinization and of the spreading of recharged surface waters, (ii) research into the behavior of pollutants in infiltrated surface waters, and (iii) investigation of hydroecological conditions which worsened due to dessication or eutrophication.

Some of the deeper wells constructed after 1970 have been equipped with many resistivity sensors to facilitate monitoring of the fresh/salt interface. Also, geophysical borehole logs were made directly after drilling to provide detailed images of the salinity gradient, while above ground geo-electrical surveys in the 1960s to 1980s filled up some spatial gaps.

Since the late 1970s multilevel observation wells were installed on various sites for detailed hydrochemical profiling, using 25–30 miniscreens in wells 25–35 m deep. Research since the 1980s followed strict sampling, preservation and analytical protocols (Stuyfzand 1993).

Groundwater recharge

Observations

Lysimeter station Castricum was constructed in 1936–1940, after which a period followed of 60 years of intensive monitoring of meteorogical parameters, gross precipitation (P), drainage quantity (Q = groundwater recharge R) and drainage quality. Some of the hydrological (and hydrochemical) results were evaluated by among others Penman (1967), Minderman and Leeflang (1968), Tollenaar and Rijckborst (1975), Stuyfzand (1987, 1993) and Stuyfzand and Rambags (2011).

The vegetation of mega-lysimeters 1–4 is more or less representative for large parts of the coastal dunes, with bare sites more frequently occurring close to the coast, dune shrub more in the central parts and the trees most inland. Important to notice that the groundwater table within the lysimeters can only fluctuate between 2.25–2.50 m below ground surface (no groundwater when 2.5 m). This limitation does not hold outside the lysimeters.

The hydrological year, defined as a period of 12 consecutive months with the best correlation between gross precipitation and discharge, appeared to be for the lysimeters the period March–February (Stuyfzand, 1986).

Hydrological maturity was attained in 1953, because since then the hydrological effects of continued growth of vegetation on lysimeters 2–4 did not affect the P-Q relationship any more, mainly because growth was compensated for by periodical thinnings. The vegetation was planted or seeded in 1940–1941, and in 2000 it was 3.5 (lys.2), 12 (lys.3) and 18 m (lys.4) high. Thinnings were most intensive on lys.4, where the number of pines gradually reduced from 700 in 1941 to ~25 in 2000.

The most important hydrological results are displayed in Fig.2, showing the logarithmic P-Q relations for the 3 vegetated lysimeters since hydrological maturity (46 years), and for the bare lysimeter since the start (56 years). These relations are based on regression analysis with P measured in the open field (both near lys.1 and at the pumping station; Fig.1). They strictly hold for hydrological years, thus without further refinements to account for delayed drainage after long dry periods.

Modeling

The 4 relations in Fig.2 have been extended to cover 7 more types of dune vegetation cover, all together forming a 1–11 scale (Table 1) with increasing evapo(transpi)ration losses and evapoconcentration of solutes (P/R). The additional 7 relations were obtained by extrapolation of data from small lysimeters (1 × 1 m, 1–4 m deep) operated in various dune areas in the period 1920–1970 and from literature data (Bakker 1981; Stuyfzand 1993).

The annual groundwater recharge under vegetation cover N (1–11) is estimated, for hydrological years (March–February), by the following equation:

$$R_N = p_N \ln(P) - c_N \qquad (1)$$

where: R_N = annual groundwater recharge under vegetation type N [mm/a]; P = annual gross precipitation in open field [mm/a]; p_N, c_N = constants for vegetation type N as defined in Table 1 [−].

Effects of climate change and changes in vegetation cover

In the Netherlands, Climate Change (CC) is expected by KNMI (2015), in the worst scenario for the years 2050 and 2085 AD, to increase annual air temperature, gross precipitation (P), evapotranspiration (E) and sea level as indicated in Table 2. The prediction for groundwater recharge (R = P-E) therefore remains close to constant, if exclusively dictated by meteorological conditions, and if seasonal changes in the timing of rainfall and evapotranspiration are ignored. However, vegetation cover is likely to change, either by increased summer droughts, forest fires, invasion of exotic species or increased attempts to reduce biomass in the eutrophying dunes. Those changes are far more decisive in what will happen to R!

Eq.1 and Table 1 offer a rapid way to estimate what may happen if a specific vegetation change is aimed at or predicted, while accepting the predicted average *P* value. For instance, an increase of P from 850 in 1995 to 918 mm/a in 2100 together with a mean decrease of vegetation from type 6 to 4, would yield an increase of R from 340 to 542 mm/a. This specific estimate is, of course, handicapped by lack of knowledge of the combined effects of among others the rise of atmospheric CO_2 concentration, and the climate change induced temperature rise, with changes in vegetation and seasonal rainfall distribution.

Fresh water lenses

Observations

Fresh water lenses in coastal environments can be classified on the basis of their shape and boundary conditions (Fig.3). Annular systems do not occur in the Netherlands, they can be found on atolls. In the Netherlands, most systems in coastal dunes are elongated, asymmetrical, semi-forced and either isolated or salt-nested (Table 2). Their size and shape have been explored since the early 1900s, when the phreatic groundwater reserves were depleted and became insufficient. A very compact summary of these investigations is shown in Table 3, together with important boundary conditions.

Fig. 2 Plot of annual totals of lysimeter discharges versus the annual total of gross precipitation, for all hydrological years (March–February) in the period 1953–1998 (lys.2–4) and 1943–1998 (lys.1)
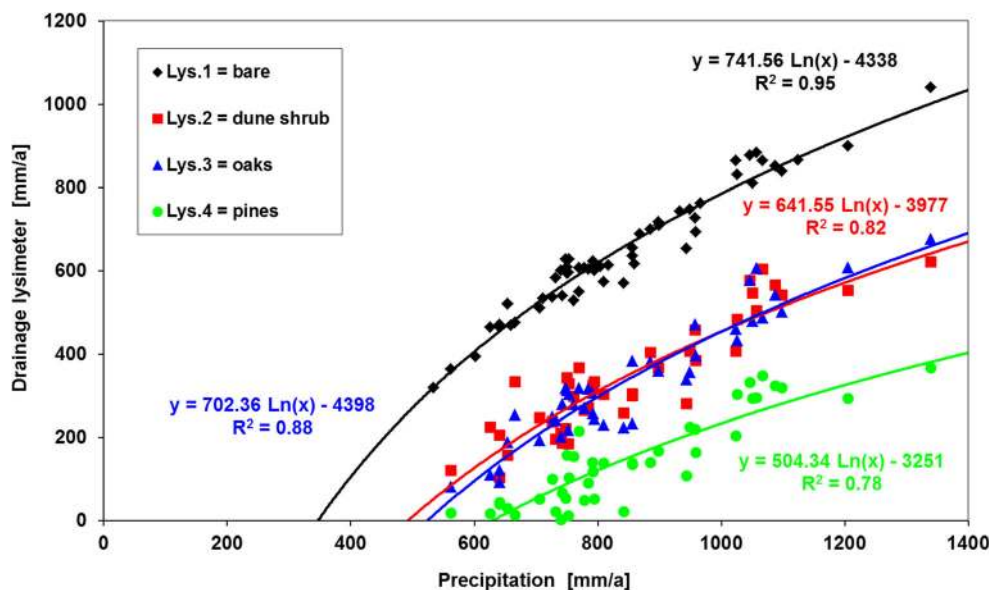
Observations on the growth rate of a fresh water lens and the mixing zone between fresh and salt groundwater are integrated with their modeling results and discussed there.

Modeling symmetrical, free, isolated lenses

The position of the groundwater table and subterranean fresh/salt interface can be calculated on the basis of simple 2D analytical approximations, which build on the Dupuit-Ghyben-Herzberg principle of fresh groundwater floating on stagnant salt groundwater (Fig.4). When equilibrium has been reached (steady state; t = ∞), this principle states (Ghyben 1889; Herzberg 1901):

$$H = \alpha h \text{ with } \alpha = \rho_F/(\rho_S - \rho_F) \tag{2}$$

where: H = depth to sharp fresh-salt water interface in equilibrium (time = ∞) [m BSL]; h = elevation of groundwater table in equilibrium [m ASL]; ρ_F = density of fresh water in lens, normally 1.000 [kg/L]; ρ_S = density of saline groundwater below lens [kg/L].

The following equation relates water density (ρ in kg/L) to EC [μS/cm at 20 °C] and temperature t [°C] at 1 atm

Table 1 Annual groundwater recharge (R) for Dutch coastal dunes as function of gross precipitation (P) and vegetation cover (N), in order of increasing (evapo)transpiration (E). Based on Fig.2 and additional data.

Evapoconcentration factor = factor with which solute concentration increases due to evapotranspiration

Vegetation			Recharge				Evapoconc
Type		Code	R = p ln(P)-c			R [mm/a]	factor
	Prec (P) mm/a =	918	p	c	E/P		fE = P/R
Bare		1	750.0	4330	0.143	787	1.167
Bare + some mosses/grasses	Lys 1	2	741.6	4338	0.215	721	1.273
Mosses		3	730.0	4360	0.324	620	1.480
Poor dry dune veg, mix of mosses + grasses + bare		4	720.0	4370	0.410	542	1.694
Dry shrubs (open), <50 % mosses/grasses		5	710.0	4383	0.498	461	1.992
Rich dry dune veg, Heather, Dry deciduous	Lys 3	6	702.4	4398	0.571	394	2.332
Dense shrubs, Wet tall grasses	Lys 2	7	641.6	3977	0.565	400	2.296
Wet dune slack, Deciduous forest (wet)		8	600.0	3750	0.626	343	2.674
Pines, dense dry		9	550.0	3500	0.725	252	3.640
Pines	Lys 4	10	504.3	3251	0.793	190	4.839
Pines, wet and dense		11	475.0	3100	0.847	141	6.532
Open water		11	475.0	3100	0.847	141	6.532

Table 2 Climate change projections for the year 2050 ± 15 and 2085 ± 15 (worst case scenario) by KNMI (2015), with 30 years averages for 1950–1980 and 1980–2010, and extrapolated values for 2100 AD

Parameter	code	unit	1950–1980	1980–2010	2036–2065	2071–2100	2100
Air temp.	t	oC	9.2	10.1	12.4	13.8	14.4
Gross precipitation	P	mm	774	851	894	911	918
Evapotranspiration #	E	mm	534	559	598	615	622
Groundwater recharge	R	mm	240	292	295	296	296
Sea Level	NAP $	m	-0.04	0.03	0.30	0.63	0.77

= Makkink, potential E for grass $ = Dutch ordnance datum

pressure, for EC ≤ 100,000 uS/cm and temperature $t = 0$–100 °C (Stuyfzand 2012):

$$\rho = 1000.3105 \, EXP(5.26 \, 10^{-7} EC) * \{1.2899 \, 10^{-12} t^5 - 4.4881 \, 10^{-10} t^4$$

$$+ 6.8771 \, 10^{-8} t^3 - 8.4536 \, 10^{-6} t^2 + 6.2538 \, 10^{-5} t + 0.9999\}$$

$$(3)$$

The ratio H/h for standard mean ocean water with $\rho_S = 1.025$ becomes 40, whereas for the Netherlands with coastal North Sea water often being 1.020–1.021, a value of 47–50 would be expected.

The analytical approximations imply a uniform, constant natural recharge of the land surface, a simple morphology and geometry of the strip of land recharged by precipitation, a homogeneous, isotropic aquifer system, a sharp fresh-salt water interface, and steady, uniform salt water conditions (Fetter 1972; Bear 1979; Vacher 1988). In reality, such conditions are never met. Aquitards are frequently observed in the aquifer system, which reduce the depth to the fresh/salt interface (H) as predicted by Eq.2, and raise h (Fig.4).

Two ideal cases are frequently discerned for free fresh groundwater lenses on saline groundwater: an infinite elongate (strip) island or coastal barrier, and a perfectly circular island. For these systems, the analytical solutions according to for instance Fetter (1972) read:
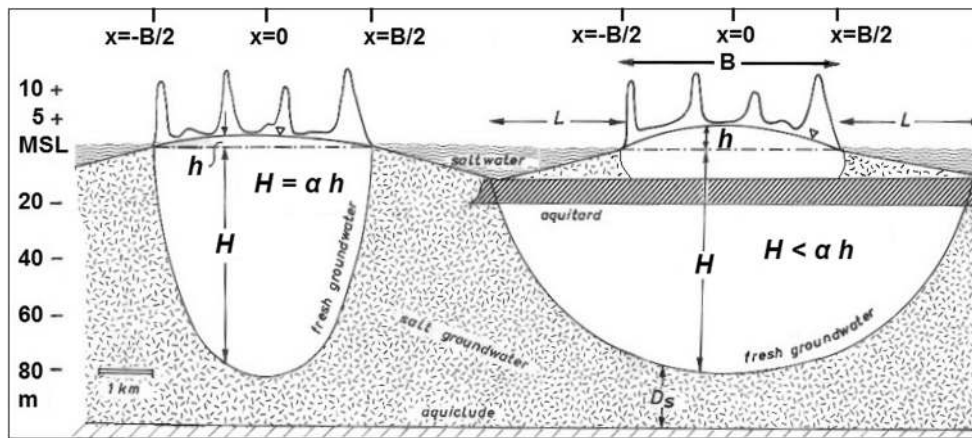
$$H_X = \surd\{R \left(0.25 \, B^2 - X^2\right)/(K \left(1 + \alpha\right))\} \qquad \text{Elongate (4A)}$$

$$H_X = \surd\{0.5 \, R \left(r^2 - X^2\right)/(K \left(1 + \alpha\right))\} \qquad \text{Circular (4B)}$$

where: R = groundwater recharge [m/d]; B = width of elongate strip of land [m]; r = radius of circular island [m]; X = horizontal distance from central axis of elongate strip of land
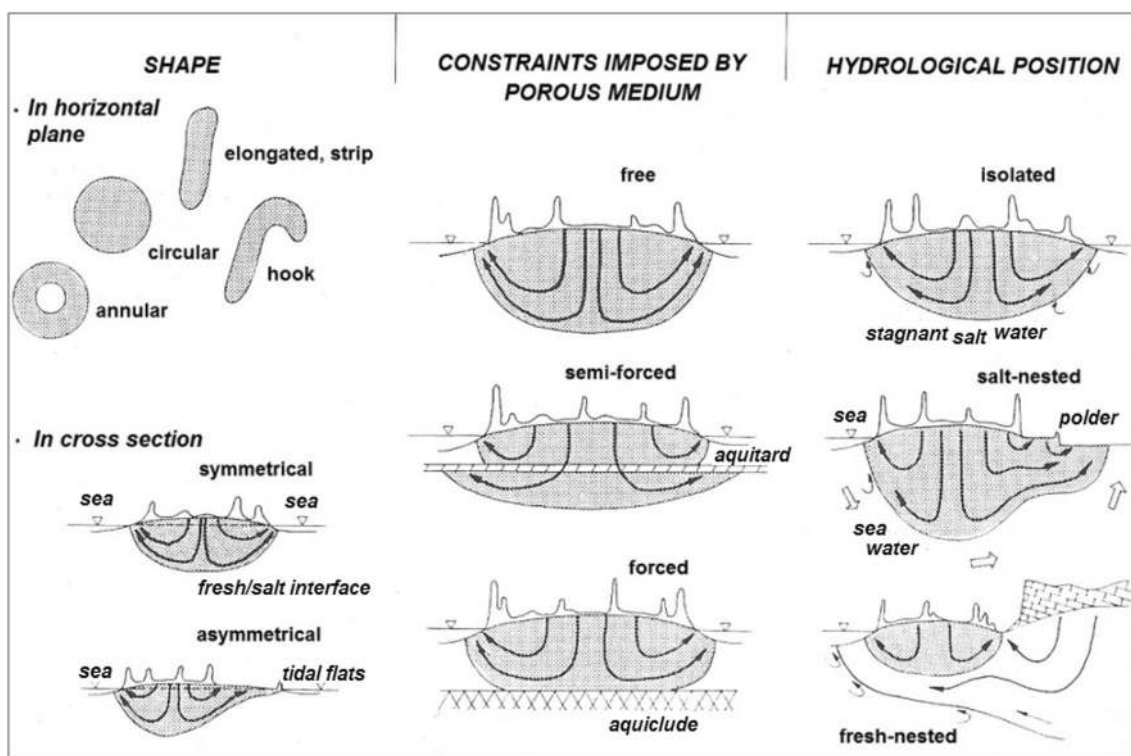
Fig. 3 Classification of coastal dune groundwater flow systems, on the basis of their shape and several boundary conditions. From: Stuyfzand (1993)

Fig. 4 Left: The Ghyben-Herzberg principle of free fresh groundwater floating on stagnant salt groundwater (Eq.2). Right: The more realistic geometry of a fresh water lens (although exaggerated), with a shallower depth to the fresh-salt water interface in equilibrium (H) than predicted (Fig.4) or from the elevation of the groundwater table (h), due to vertical flow and anisotropy of the porous medium ($K_h > K_v$). L = length of fresh water tongue; D_S = thickness of aquifer system saturated with salt water. Slightly modified from Stuyfzand 1993

(Fig.4) or from center of circle [m]; K = mean hydraulic conductivity of aquifer system [m/d].

h_X is calculated from H_X via Eq.2. Important to notice is that K strongly depends on (water) temperature, due to fluid density and viscocity effects, according to Olsthoorn (1982):

$$K_{t2} = K_{t1}\frac{\nu_{t1}}{\nu_{t2}} = K_{t1}\frac{(t_2 + 43.1)^{1.502}}{(t_1 + 43.1)^{1.502}} \qquad (5)$$

where: K_{t1}, K_{t2} = mean hydraulic conductivity of aquifer system at temp = t_1 and t_2 (°C), respectively [m/d]; ν_{t1}, ν_{t2} = kinematic viscosity of water at temp = t_1 and t_2, respectively [m²/s].

The time needed to form a fraction (p) of the fresh groundwater lens in equilibrium (t_P in days), i.e. the growth curve, is approximated by equations given by Huisman and Olsthoorn (1983):

$$t_P = \text{Atanh}\,(p)/\sqrt{\left\{(4\,K\,R)/\left[(0.25\,\pi\,\varepsilon\,B)^2\rho_S/(\rho_S-\rho_F)\right]\right\}} \qquad \text{Elongate} \quad (6A)$$

$$t_P = \text{Atanh}\,(p)/\sqrt{\left\{(4.5\,K\,R)/\left[(\varepsilon\,r)^2\rho_S/(\rho_S-\rho_F)\right]\right\}} \qquad \text{Circular} \quad (6B)$$

where: Atanh (p) = inverse of tangent hyperbolic of $p = 0.5$ ln $\{(1+p)/(1-p)\}$; p = fraction of full grown fresh groundwater lens = $H_{t=t}/H_{t=\infty}$ [0 - <1]; ε = effective porosity [−].

As an example, Fig.5 shows how h, H and $t_{0.99}$ depend on the width (B) of an elongate dune strip, under the indicated conditions. The relations are nearly linear.

The predicted and observed growth curve of a freshwater lens is shown in Fig.6 for a low lying sandy strip island (Veermansplaat; site 20 in Table 3), situated in a saline estuary (Grevelingen) that was closed off from the sea in 1970 by a dam, while maintaining a rather constant salinity of 16,200 mg Cl/L and being excluded from tidal effects. Eq.6A performs very well not only on site 20 (B = 475 m),

but also in the small sized sand tank experiments (0.8 m) by Stoeckl and Houben (2012).

The age distribution within a steady state, fully developed lens differs from the one during continued growth (Eq.6), because during steady state all flow is directed towards the exfiltration sides, thus extending most flowlines and increasing the age. The age depth distribution can be approximated for a steady state dune strip by applying the following equation (Eq.18 in the Appendix of Stuyfzand and Bruggeman 1994) to selected distances (X) within the width of the lens, after replacing z by z' = z H_X / H_0 with z and H downward positive [m]:

$$t_{Z'} = \frac{\varepsilon B}{2\sqrt{R(\alpha K_h + R)}}\ln\left(\frac{B\sqrt{R}}{-2Z'\sqrt{\alpha K_h + R} + B\sqrt{R}}\right) \qquad (7)$$

The groundwater travel time equation for a strip island with a free, isolated lens, as presented by Chesnaux and Allen (2008) and Greskowiak et al. (2012), yields practically identical results. The stratification pattern of groundwater ages as depicted in Fig.7 was confirmed by sand tank experiments by Stoeckl and Houben (2012). Field evidence of groundwater age stratification in coastal dunes is available from Stuyfzand (1993), Röper et al. (2012) and Houben et al. (2014).

Modeling symmetrical, semi-forced, isolated lenses

In reality, the presence of intercalated aquitards may strongly disturb the H/h ratio (Fig.4-5), by increasing h and t_{99} in a stable lens (over time), and decreasing H. In addition, a submarine fresh water tongue will form below the aquitard (Fig.4) with length L. The length of this tongue can be estimated for a free water lens by Van der Veer (1977) and for a semi-forced lens by Bakker (2006), but good field data for verification of their methods are lacking.

Fig. 5 Calculated effects of size of an elongate, symmetrical fresh water lens on maximum groundwater table (h_0), maximum depth to the fresh-salt interface (H_0), and 99 % formation time of a fresh water lens (t_{99}), with and without intercalated aquitard with resistance $c_V = 1500$ d. Conditions: $R = 0.40$ m/a, $K = 6.2$ m/d, $\varepsilon = 0.35$ en $\alpha = 50$. Arrows indicate the changes due to the aquitard's presence (see Eqs. 8–11)
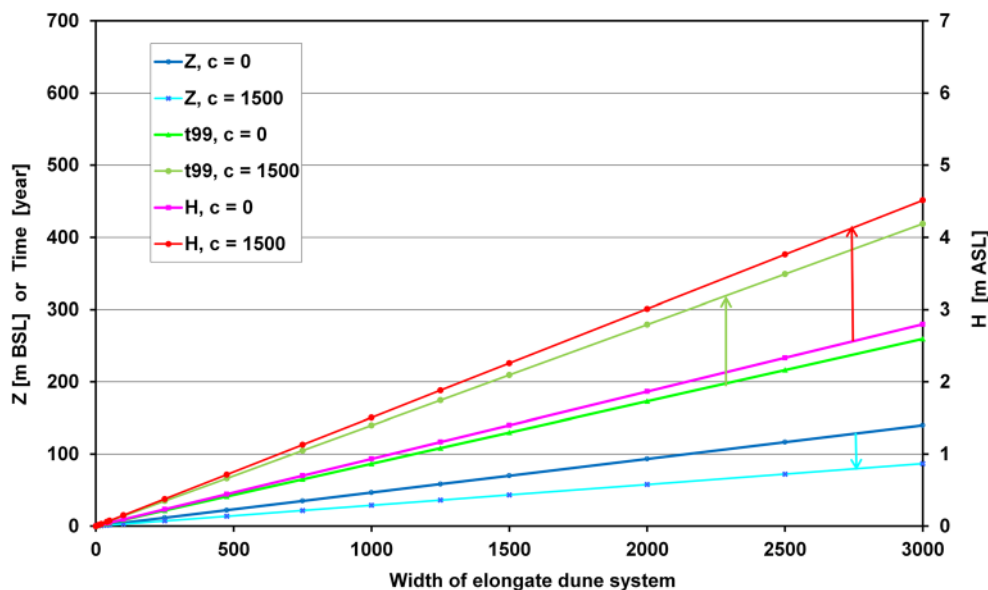
The increase of h and t_P, and decrease of H as function of the hydraulic resistance to vertical flow (c_V) can be estimated as follows, on the basis of the observed H/h ratio of many fresh water lenses in the Dutch coastal dune area prior to large scale groundwater abstraction (Table 3):

$$h_C = f_C h \quad (8)$$

$$H_C = H/f_C \quad (9)$$

$$t_{P,C} = f_C t_P \quad (10)$$

with:

$$f_C = 5 - -4 EXP(-c_V/9000) \quad (11)$$

Fig. 6 Calculated (Eq.6A) and observed growth curve of a fresh water lens on a free strip island that emerged permanently above the surrounding saline lake water when the Grevelingen estuary was closed off from the sea in 1970 by a dam (from Stuyfzand et al. 2014). H = depth to fresh/salt interface being 8100 mg Cl/L. Conditions: B = 475 m, $R = 0.20$ m/a, $K = 6.2$ m/d, $\varepsilon = 0.35$ and $\alpha = 50$

The factor f_C varies from 1 (zero vertical flow resistance) to 5 (high c_V). Effects of these corrections are also shown in Fig.5, for $c_V = 1500$ d.

The factor f_C can be tested against observations (Table 3) by comparing the observed ratio H/h with the calculated ratio $H_C/h_C = \alpha / (f_C^2)$. The relation between both is quite satisfactory ($R^2 = 0.88$), if realized that the data in Table 3 are to some degree biased by effects of (i) pumping, forestation, urbanization or land reclamation inland; (ii) coastal retreat or progradation; (iii) flow parallel to the coast; and (iv) discontinuity or heterogeneity of the main aquitard. Also, the c_V of only the main aquitard separating the phreatic from the semi-confined aquifer was taken (mostly based on reported pumping tests), thus excluding effects of deeper aquitards within the fresh water lens (if present). Their inclusion, however, worsened the performance of the calculated ratio, so they were left out.
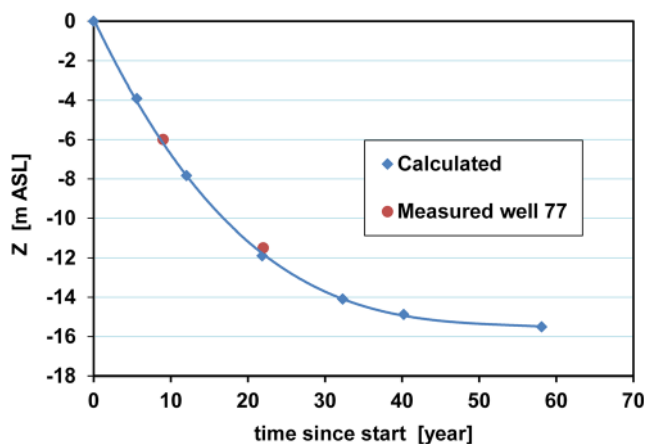
Modeling symmetrical, forced lenses

When the fresh water lens in a phreatic aquifer is resting on an impermeable base (aquiclude), then the situation becomes as depicted in Fig.8 and as discussed by Fetter (1972) and Vacher (1988). Bakker (1981) presented the following solution for a strip island (his factor 40 replaced here by α), in which the inland salt water tongues (L_S) are playing an important role:

if

$$-(§B-L_S) \leq X \leq §B-L_S : \quad h_X{}^* = \sqrt{\frac{R(0.25B^2-X^2)}{K} + \left(\frac{\alpha+1}{\alpha}\right)H_0{}^2} \quad (12)$$

with

$$L_S = 0.5B - \sqrt{\frac{B^2}{4} - \frac{K(1+\alpha)H_0{}^2}{\alpha^2 R}} \quad (13)$$

Table 3 Inventory of size, shape and hydrological position of fresh water lenses along the Dutch North Sea coast, with data on the vertical hydraulic resistance (c_V) of the main aquitard ($c_V = d/K_V$ where d = thickness of aquitard, K_V = vertical hydraulic conductivity), Cl concentration ($Cl_S$) and density of surrounding saline groundwater (ρ_S), the observed H/h-ratio and the corrected H_C/h_C-ratio calculated by combining Eqs.2, 8, 9 and 11. h_0, H_0 = height of groundwater table and depth to fresh/salt-interface at x = 0 (in the middle of the lens), respectively [m Above Sea Level]

Coastal dune area		h_0	H_0	Shape	Hydrol. position	Aquitard	Cl_s	P_s	H/h	H_C/h_c	Data in
Figure 1	Name	m ASL				$c_{v\ [d]}$	mg/L	kg/L	observed	calc.	Ref #
1	Schiermonnikoog	4	-90	circ, island	isolated	700	17,400	1.022	23	27	a
2	Ameland (east)	3	-60	strip, island	isolated	1000	17,400	1.022	20	23	a
3	Ameland (west)	3	-50	circ, island	isolated	4000	17,400	1.022	17	8	a
4	Terchelling (east)	3.5	-80	strip, island	isolated	2500	17,400	1.022	23	12	a
5	Terschelling (mid)	3	-50	strip, island	isolated	2500	17,400	1.022	17	12	a
6	Terschelling (west	5	-100	circ, island	isolated	1250	17,400	1.022	20	20	a
7	Vlieland	3.5	-45	strip, island	isolated	2000	17,400	1.022	13	14	a
8	Texel	4	-60	strip, island	isolated	1500	17,400	1.022	15	18	b
9	Zwanenwater	2.7	-25	strip, main	salt-nested	10,000	16,500	1.020	9	4	c
10	Schoorl	9	-135	circ, main	salt-nested	3000	17,000	1.021	15	10	d
11	Egmond aan Zee	7	-40	strip, main	salt-nested	15,000	16,800	1.021	6	3	d
12	Castricum	3	-120	strip, main	salt-nested	200	16,300	1.020	40	42	d
13	Wijk aan Zee	8	-55	strip, main	salt-nested	10,000	16,200	1.020	7	4	d
14	Kennemerduinen	6	-140	strip, main	salt-nested	1000	16,500	1.020	23	24	d
15	Amsterdam dune catchment	7	-120	strip, main	salt-nested	3000	16,700	1.021	17	11	d
16	Berkheide	8	-80	strip, main	salt-nested	5000	16,500	1.020	10	7	e
17	Meijendel	5	-120	strip, main	salt-nested	1000	15,500	1.019	24	26	e
18	Monster	4	-55	strip, main	salt-nested	5000	10,000	1.012	14	11	f
19	Goeree (Westduinen)	2	-35	strip, island	isolated	5000	15,000	1.019	18	7	g
20	Veermansplaat	0.35	16	strip, island	isolated	0	16,200	1.020	46	50	b
21	Schouwen	7	110	circ, island	isolated	3000	14,800	1.018	16	12	i

a = Beukeboom 1976, b = Stuyfzand et al. 2014, c = Stuyfzand and Lüers 1992, d = Stuyfzand 1993, e = Stuyfzand et al. 1993, f = Beijerinck et al. 1909, g = Bakker 1981, i = Van Oldenborgh 1916

Fig. 7 Calculated shape (defined by h = water table, and H = depth to fresh/salt interface) of a steady state, fresh water lens on a strip island with isochrones of travel time (3–127 years). The isochrones 3–64 coincide with the 10–90 % depth H_X of the lens, 83 and 127 with the 95 and 99 % depth. Conditions: B = 475 m, K = 6.2 m/d, ε = 0.35, R = 0.20 m/a, ρ_F = 1.000, ρ_S = 1.020 kg/L
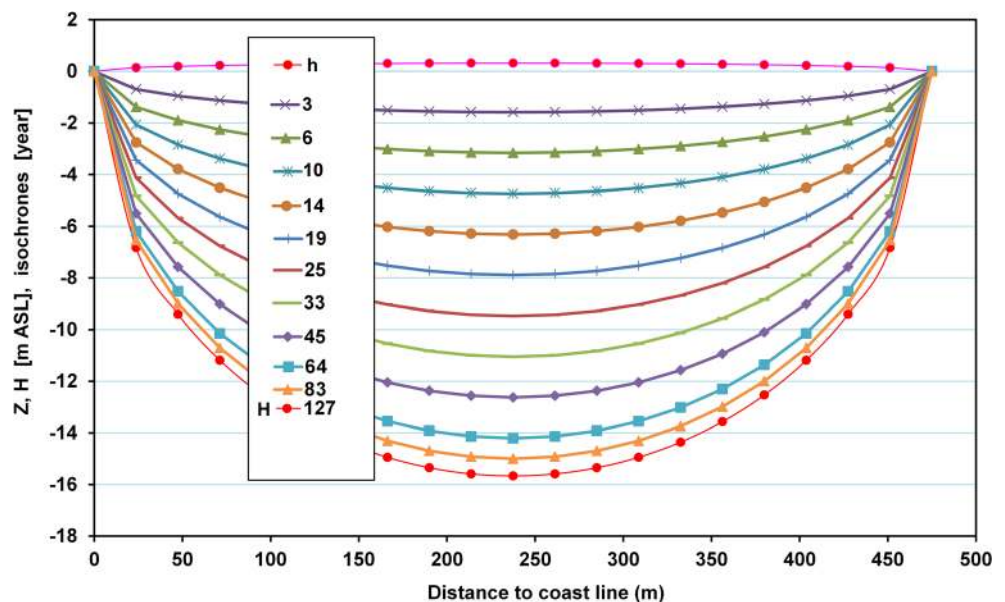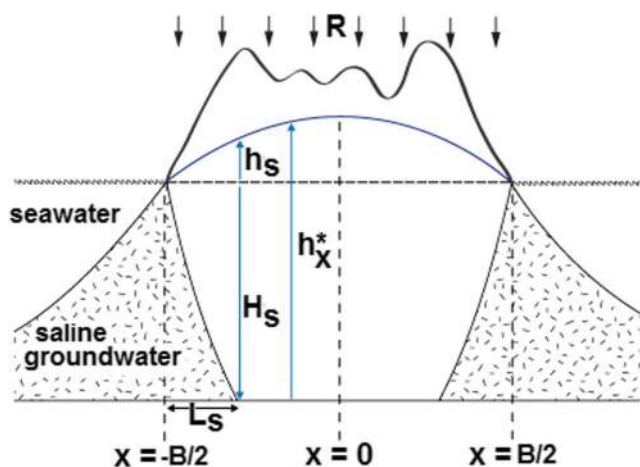
Fig. 8 Schematic of a forced freshwater lens on a strip island resting on a horizontal impermeable base (aquiclude)

Fig. 9 Dispersive mixing between fresh (F) and salt (S) groundwater, in case of a steady position of both fluids, an equal flow velocity and direction, an isotropic medium and no mixing at the starting point of flow (adapted from Verruijt 1971)

where: $h_X^* = h_X + H_S$ [m] (Fig.7); $H_S = H_0$ [m BSL].

Eqs. 2 and 4A hold again where $\{-\tfrac{1}{2}B \leq X \leq -\tfrac{1}{2}B + L_S\}$ and $\{\tfrac{1}{2}B - L_S \leq X \leq \tfrac{1}{2}B\}$.

Modeling the transition zone

Where fresh and salt groundwater meet, or dune groundwater and infiltrated Rhine River water (see later section), always a mixing zone between both water types will form. In case of stagnant waterbodies the mixing is driven by diffusion, and in case of flowing waterbodies it is mainly driven by dispersion. Even if the surrounding saline groundwater is (quasi)stagnant on a large scale (ignoring tidal effects), along the interface this water is dragged in the flow direction of the fresh water, so that transversal dispersion becomes the main mechanism. Bear and Todd (1960) and Verruijt (1971) simulated the transversal dispersion across a steady interface of two fluids moving at equal velocity in the same subhorizontal direction in an isotropic aquifer, with zero mixing at the starting point of flow (Fig.9) as follows:
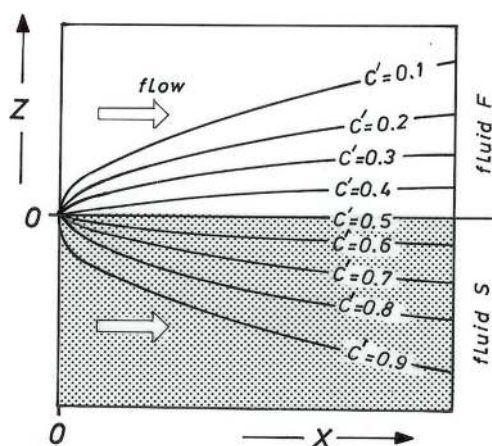
$$C'_{X,Z} = 0.5 \left(1 - erf\left(\frac{z}{2\sqrt{\alpha_T X}}\right)\right) \qquad (14)$$

with

$$C' = (C - C_F)/(C_S - C_F) \qquad (15)$$

And where:

$C'_{X,Z}$ = the relative concentration C' of conservative tracer C as a function of X and z; C_F, C_S = absolute concentration of conservative tracer C in fluid F and S respectively [mg/L]; X = total distance travelled in the direction of parallel flow [m]; z = shortest distance to the interface, upward positive [m]; erf = error function (max = +1; min = −1; [−]); α_T = transversal dispersivity [m].

In a symmetrical lens, the starting point for both seaward and inland flow is situated right in the middle at X = 0. For practical reasons, the mixing zone can be delineated by C′ = 0.01 and C′ = 0.99, which implies a transition from 195 to 16,340 mg Cl/L when dealing with fresh and salt water of 30 and 16,500 mg Cl/L, respectively. The value C′ = 0.01 implies that erf $\{z/[2\sqrt{(\alpha_T X)}]\}$ be 0.98 (Eq.9), which is true if erf $\{z/[2\sqrt{(\alpha_T X)}]\}$ equals 1.645. This means z = 3.29 $\sqrt{(\alpha_T X)}$, and the total width of the symmetrical transition zone (D_{1-99}) now becomes, in m:

$$D_{l-99} = 6.58\sqrt{(\alpha_T X)} \qquad (16)$$

Other boundaries can be applied for the transition zone, for instance when comparing calculations with field observations, such as $D_{10-90} = 3.60\sqrt{(\alpha_T X)}$, $D_{20-80} = 2.39\sqrt{(\alpha_T X)}$, etc.

As an example, 2 chloride logs are presented in Fig.10, one close to the deep groundwater divide at that time (750 m seaward in 1912) and the other about 1500 m seaward. An excellent agreement is obtained with the calculated transition zone for well 19 A.19, using Eq.14 with X = −750 m, α_T = 0.01 m and 30 and 17,000 mg Cl⁻/L for the fresh dune and salt North Sea end members. Discrepancies between the observed and calculated log for well 19 A.18 can be attributed to residual brackish groundwater in a local clay layer at 45–64 m BSL, and an overall slightly lower hydraulic conductivity and higher dispersivity than around 19 A.19.

The calculated, extremely thin zone below and fringing the deep groundwater divide (Fig.9), does not match with observations (Stuyfzand 1993). Longitudinal dispersion during vertical flow (which is dominating there) and changes in the position of the groundwater divide and water table are likely responsible for this.

Fig. 10 Comparison of observed and calculated Cl logs for two piezometer nests in coastal dunes north of Bergen (area 10 in Fig.1) in 1912, before the onset of deep dune water exploitation (From: Stuyfzand 1993). Observations on piezometers with a 1 m long screen. Calculations are based on Eq.16, using $\alpha_T = 0.01$ m, X = −750 m for 19 A.19 and −1500 m for 19 A.18, 30 mg Cl/L for fresh dune water and 17,000 mg Cl/L for salt North Sea water. BSL = Below Sea Level. Dune system: B = 5000 m, $R = 0.37$ m/a, K = 6.2 m/d, $\varepsilon = 0.35$
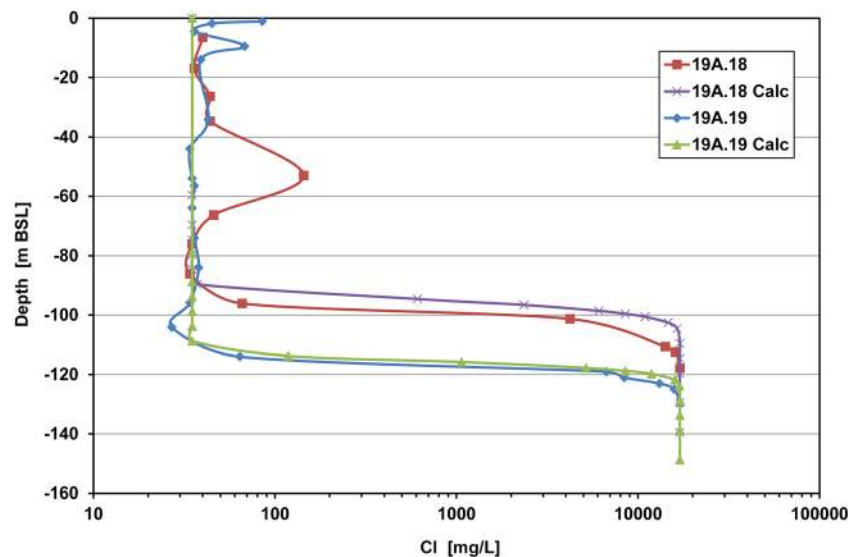
Effects of sea level rise with coastal erosion

In the following we assume that sea level rise (SLR) will lead to inundation of land along the coast according to the existing topography, without countermeasures by man and without natural adaptation of the coastline. SLR then leads to a direct reduction of the area above sea level where rainwater previously recharged the fresh water lens. The inherent shoreline retreat (SOR; m) can be approximated as follows:

$$SOR = SLR/I_T \tag{17}$$

where: SLR = Sea Level Rise [m]; I_T = seaward slope of beach [−].

This retreat leads to a decrease in width of the recharge belt, which reduces the width of an elongate strip (B) or the radius of a circular island (r), thereby leading to a smaller size of the fresh water lens after equilibration to the new situation. The new situation can be easily calculated with Eqs.2–17 by taking: $B_{SLR} = B - SOR$ for a coastal dune strip system bordered on one side by the sea and on the other side by not inundated marsh land or a polder; $B_{SLR} = B - 2$ SOR for a coastal dune strip bordered on both sides by the sea; and $r_{SLR} = r - SOR$ for a circular island. The parameters B_{SLR} and r_{SLR} stand for B and r after SLR respectively.

The effect on the groundwater table is calculated by taking into account that base level rose by an amount equal to SLR, either on one or both sides.

The case, with a unilateral SLR and an elongate dune strip on the mainland, creates tilting of the fresh water lens, which complicates the calculations as outlined before, when aiming at more precision. The groundwater divide will shift seaward due to inland tilting of the fresh water lens (Fig.11c). This means that the seaward flow branch becomes shorter and the inland flow branch longer. The net effect of this is that more fresh groundwater is lost by transversal mixing (Fig.11c). In the simplified approximation as applied here, we calculate the depth of the fresh/salt interface H via Eq.4A with $B_{SLR} = B - SOR$ and with addition of Δh [m], which is defined as the fictive linear change in base level of the groundwater table between mean sea level and the adjacent polder level (PL; m BSL):

$$\Delta h = (SLR–PL)/\{(0.5 + X/B)\,PL + (0.5–X/B)\,SLR\} \tag{18}$$

With this new H_2 (= H + Δh) the new position of the groundwater table (h_2) is calculated by taking:

$$h_2 = \alpha\,(H_2 - \Delta h) + \Delta h \tag{19}$$

For example, if sea level would rise with 1 and 5 m respectively, where the coastal belt was 2500 m wide, sea floor inclination 7 m/km and PL = 0, then the fresh water lens would change its size and shape as indicated in Fig.11. In scenario A the coastal barrier is attached to the mainland where the saline groundwater table remains equal to the initial (current) sealevel (Fig.11a), in scenario B it is surrounded by the sea on both sides (Fig.11b). Upon sealevel rise the lens becomes salt-nested in case of scenario A, but remains isolated in case of scenario B. Under the given conditions it is calculated that in scenario A the coast will retreat on one side by 143 and 716 m respectively, and in scenario B it will retreat by these numbers on both sides. This reduces the width of the barrier system very significantly.

In scenario A the midway depth of the fresh/salt-interface (H_0) will decrease by 7 and 36 m, and the midway groundwater table (h_0) will rise with 0.37 and 1.83 m, upon an SLR of 1 and 5 m respectively. The volume of fresh groundwater (Cl =30–150 mg/L) will decrease by 12 and 55 %. In scenario B
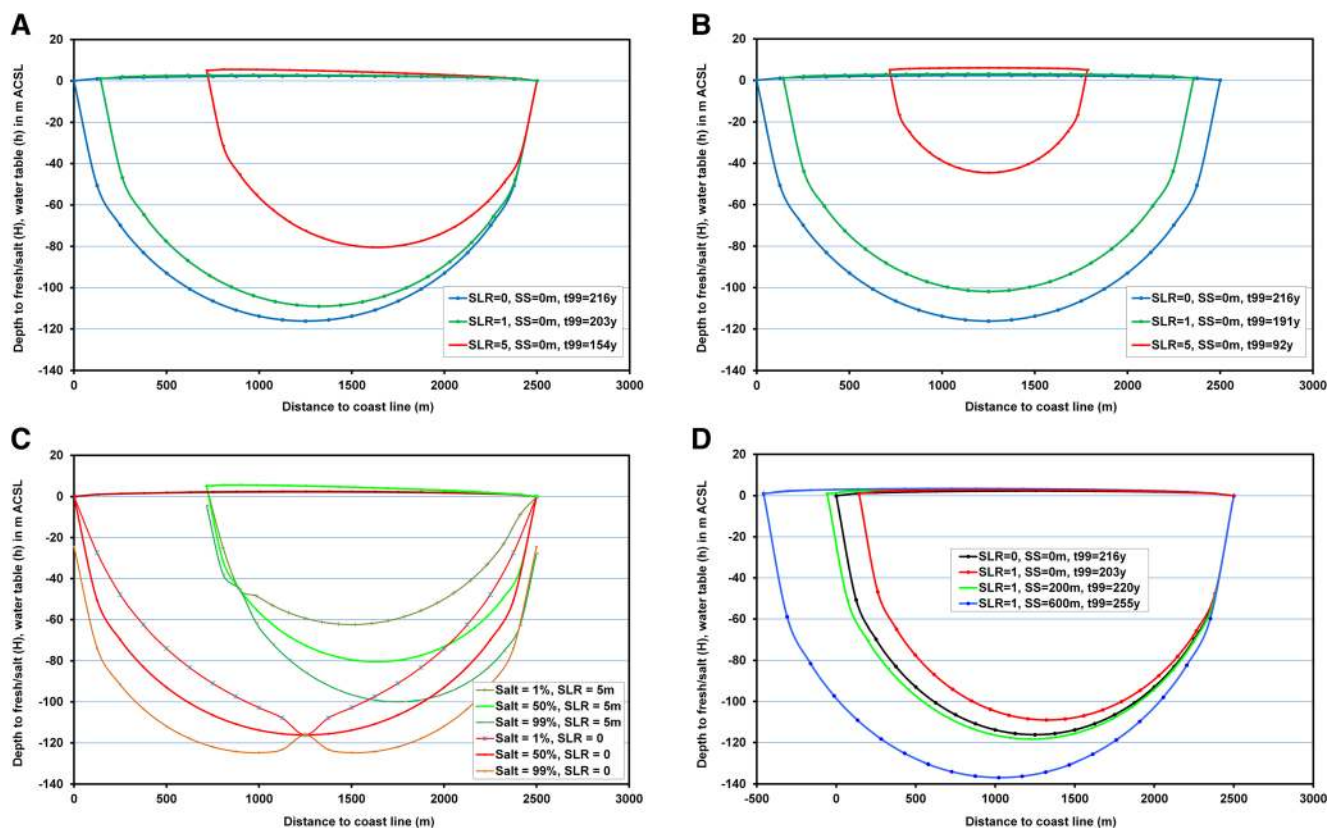
Fig. 11 Predicted shape of the fresh water lens in cross section of an elongate coastal dune system, with current sea level (0), 1 and 5 m Sea Level Rise (SLR). A: free lens in a dune system attached to the mainland on the right hand side, where saline groundwater table remains fixed at current sealevel. B: free isolated lens in a dune strip island surrounded by the sea on both sides. C: as A, excluding SLR +1 m, including mixing zone of 1–99 % seawater. D: as A, excluding SLR + 5 m, including coastal extension (SS) of 200 and 600 m by beach nourishment prior to 1 m SLR. Plotted years indicate the time needed to form the whole fresh water lens (99 %) from the beginning. ACSL = Above Current Sea Level. Conditions: B = 2500 m, K = 6.2 m/d, c_V = 0 d, ε = 0.35, R = 0.40 m/a, ρ_F = 1.000, ρ_S = 1.020 kg/L, α_T = 0.01 m

the decrease of H_0 and the rise of h_0 are about twice as much as for scenario A, while the volume of fresh groundwater decreases by 23 and 84 %.

Effects of coastal progradation

SLR may be accompanied by coastal adaptation composed of spontaneous accretion of the beach barrier and tidal flats, or by anthropogenic beach nourishment. In this section, the same 'basic' hydrogeological system is addressed as in scenario A, but now the SLR is limited to 1 m and is combined with a preventive, initial seaward coastal extension of 0, 200 and 600 m respectively, by sand nourishment. The resulting net coastal expansion then becomes −143, +57 en 457 m respectively. Under these conditions it is calculated that the fresh water lens will change its shape and size as indicated in Fig.11d.

Clearly, the overall effects of SLR and sand nourishment are most prominent along the expanding coast. The largest part of the expansion of the fresh water lens will probably take several decades, as can be deduced from the growth curve of the lenses, and the difference between t_{99} of the various lenses shown.

Effects of other environmental changes

Other environmental changes with an impact on the fresh water lens consist of changes in groundwater recharge (R), hydraulic conductivity (K), hydraulic resistance to vertical flow (c_V), and density of fresh (ρ_F) and salt (ρ_S) groundwater.

An increase of R, resulting from for instance more rainfall because of climate change (Table 2), or less evapo(transpi)ration because of decreasing vegetation, or less groundwater extraction, will lead to expansion of the lens (Eq.4).

The effects of a permeability increase when temperature rises due to either climate change (Table 2) or less vegetation (Pluhowski and Kantrowitz 1963), are more difficult to foresee, because of simultaneous effects on water viscosity and density, and the contrary effects of an increase of K (Eq.4) and decrease of c_V (Eq.8–9). Nevertheless, the effects on permeability K (Eq.5) outweigh the effects on water density (Eq.3) and c_V (Eq.5 and Eq.11), so that the lens will shrink.

An increase in the density contrast between fresh and salt water, for instance by less coastal dilution of oceanwater due to reduced river outflows, will conduce to shrinkage of the freshwater lens. The effects on hydraulic conductivity can be ignored.

Environmental changes usually are complex involving many parameters, necessitating to apply the full fledged suite of analytical solutions presented.

Neglected mechanisms

We neglected several mechanisms that may enhance or reduce the predicted effects of the scenario's modeled. For instance, the prediction of a strong rise of the groundwater table in case of SLR or sand nourishment may be counteracted by the following mechanisms: (i) the development of more vegetation which evaporates more water, thus reducing R; (ii) the genesis of (more) open water, leading to more evaporation losses and to the so-called open-water-effect; and (iii) drainage of surface water from the area, to the sea or hinterland.

These mechanisms also counteract any predicted lowering of the groundwater table.

Sea level rise may lead to coastal erosion which adds to the effects of inundation, but it may also deposit sand when sea currents and wind directions are favourable. Tectonic movements and land subsidence by clay compaction, peat oxidation or even decalcification strongly interfere with SLR; subsidence will enhance SLR effects.

Opportunities

Sand nourishment on a very large scale, such that the coastline will move seaward by many 100 s of meters, has 2 important beneficial side-effects (in addition to coastal protection against SLR). The first is that the inland hydraulic gradient of the salt groundwater under the fresh water lens is reduced. This slows down the higher salinity North Sea water intrusion, which is replacing the lower salinity, relict Holocene lagoonal groundwater (Stuyfzand 1993).

The second is that an expanding fresh water lens may reach an important aquitard, thus closing off that aquifer from lateral sea water intrusion. The lens thereby acts as a natural hydraulic barrier, at least in that aquifer.

Rainwater lenses

Observations

A nice example of a well developed rainwater lens is shown in Fig.12, where Rhine River water is flowing below the lens from the influent recharge canal towards the draining Van der Vliet canal at X = 800 m (site 15 in Table 3). The lens and transition zone between the 2 fluids (with 10–90 % mixing) are both clearly expanding downgradient. Flow-through lakes, which are numerous on sites 16–17 in between the infiltration and exfiltration

zone of riverwater, may strongly disturb a rainwater lens which is forced to exfiltrate in the lake together with the underlying river water and mix there (Stuyfzand 1993).

Discerning rainwater lenses is a matter of multitracing and using multilevel wells (with very short well screens (1–10 cm). The rainwater lens could be easily discerned from the infiltrated Rhine River water in Fig.8, by its lower Cl concentration and even more unambiguously by its lower ^{18}O and lower Cl/Br-ratio (Stuyfzand 2010).

Modeling

The thickness of a rainwater lens and its mixing zone (Fig.13) can be accurately calculated using the following set of equations (Stuyfzand and Stuurman 1985; Stuyfzand 1993):

$$D_X = \frac{R\,X}{K\left\{\dfrac{C_1\,e^{-\frac{X}{\lambda}}}{\lambda} - \dfrac{C_2\,e^{\frac{X}{\lambda}}}{\lambda} - \dfrac{\phi_m-\phi_o}{M}\right\}} \tag{20}$$

$$C_1 = H_o - C_2 - R\,c_v - \phi_o \tag{21}$$

$$C_2 = \frac{H_M - \left(H_o - R\,c_v - \phi_o\right)\,e^{-\frac{M}{\lambda}} - R\,c_v - \phi_M}{e^{\frac{M}{\lambda}} - e^{-\frac{M}{\lambda}}} \tag{22}$$

$$H_X = C_1\,e^{-\frac{X}{\lambda}} + C_2\,e^{\frac{X}{\lambda}} + R\,c_v + \phi_x \tag{23}$$

$$t_X = \int_{X=0}^{X=X} \frac{-n}{K}\left[\frac{dX}{dH}\right]dX = \sim \frac{-nX^2}{K(H_0-H_X)} \tag{24}$$

$$D_{10-90} = 3.624\,\sqrt{\alpha_T\,X} \tag{25}$$

where:

D_X = thickness of rain water lens (D_{50} = 50 % rain and 50 % river water) at distance X [m];]; D_{10-90} = thickness of mixing zone of 10–90 % river water [m]; H_0, H_M, H_X = phreatic head [m ASL] at distance X = 0, X = M, X = X respectively; K = horizontal permeability [m/d]; R = groundwater recharge [m/d]; X = distance to closest bank of relevant spreading basin, as measured in horizontal plane along flow line [m]; M = as X but any point beyond X = 0 where H and φ were measured; C_1, C_2 = integration constants defined by boundary conditions; c_v = vertical hydraulic resistance of aquitard = (Z_1-Z_2)/K_V [d] with K_V = vertical permeability [m/d]; λ = √(K$D_A$$c_V$) = leakage factor [m]; D_A = −Z_1+ ½(H_o + H_x) ∼ mean thickness of upper aquifer [m]; φ_0, φ_X = piezometric head in second aquifer at X = 0 and X = X [m ASL]; Z_1, Z_2 = position of aquitard top and base, respectively [m ASL]; α_T = transversal dispersivity of porous medium [m]; n = effective porosity [−]; t_X = travel time of water from X = 0 to X = X in phreatic aquifer [d].

Fig. 12 Observed rainwater lenses in the Amsterdam dune catchment area (site 15 in Fig.1), where Rhine River water is recharged artificially since 1957 (modified from Stuyfzand 1993). Lens i = ill developed due to fast flow between basin 1 and draining Barnaart canal; Lens ii = moderately well developed because of little flow between basin 1 and supply canal; Lens iii = well developed thanks to slow flow and long transit time (ca. 17 years) between supply canal and draining Van der Vliet canal. MSL = Mean Sea Level. a = silty fine sand; b = silty clay
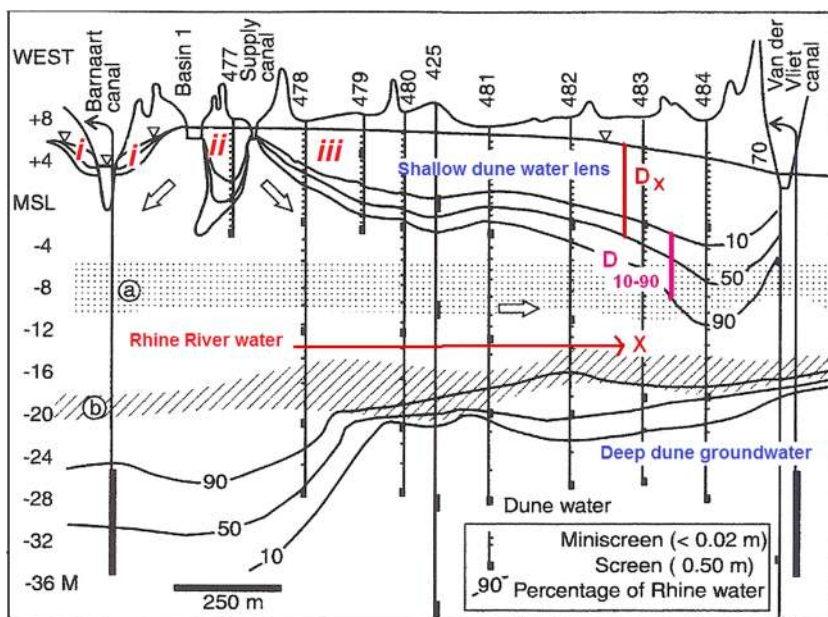
The conditions for application of Eqs.20–25 are: steady state, $X \geq 0$, (sub)horizontal flow (Dupuit), $\varphi_X = a + bX$ (a, b = constant), $D_X < (-Z_1 + H_X)$ and $D_A >> (H_0 - H_X)$.

The mixing zone D_{10-90} due to transversal dispersion was very well predicted by Eq.25 with a very low α_T being 0.0025 m (Stuyfzand and Stuurman 1985; Stuyfzand 1993).

Effects of climate change

The main relevant effects of CC on rainwater lenses in and around artificial recharge areas using basins, consist of a temperature increase affecting K and c_V (= $(Z_1-Z_2)/K_V$) via Eq.5, and a change of R, which mainly depends on vegetation as discussed earlier. How such changes affect D_X is shown in Fig.14. The temperature is expected to increase for Rhine River water in year 2100, by about +5 °C (+4 °C being the increase in air temperature, and +1 °C resulting from increased needs of cooling capacity).

A temperature increase clearly results in a relatively small decrease of D_X, because the riverwater with a lower viscosity will flow faster and thereby reduce the formation time of the rainwater lens. The effect will be delayed, however, by a factor ~ 1.9, which is the observed

Fig. 13 Schematic of a rain water lens on top of infiltrated Meuse River water migrating seaward, with important parameters for calculating its thickness (D_X), and the mixing zone D_{10-90} between both watertypes. For definition of parameters, see explanation to Eqs.20–25
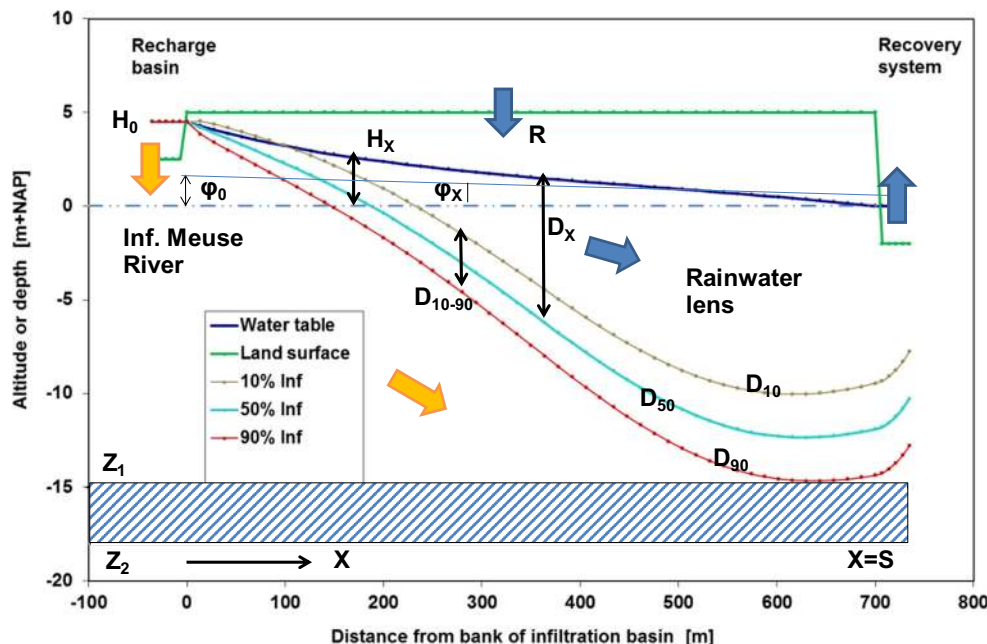
Fig. 14 Effects of temperature on the thickness of a rainwater lens (D_{50}) in an artificial recharge area, as calculated with Eqs. 5 and 20
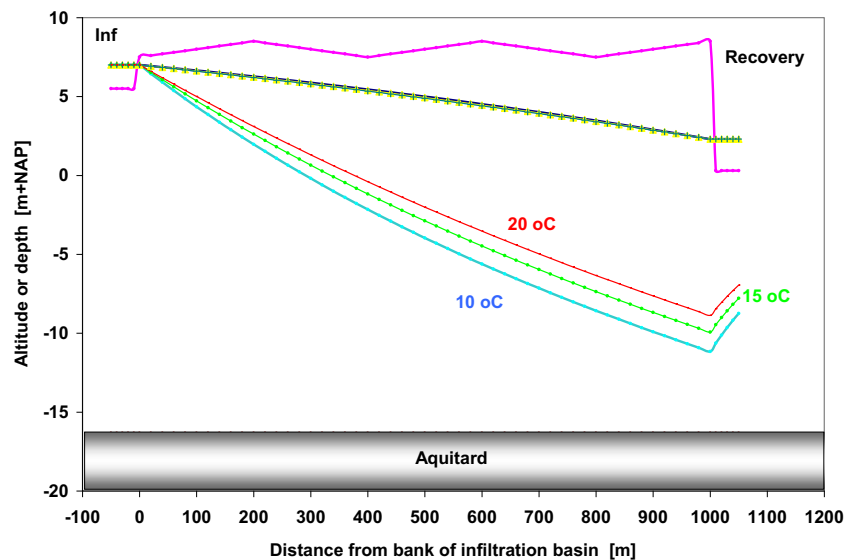
(Olsthoorn 1982) and calculated (Huisman and Olsthoorn 1983) retardation factor for temperature fronts in a sandy aquifer with porosity 0.35.

Another side-effect of CC is an expected increase in the frequency and duration of intake stops of riverwater to be pretreated and transported to artificial recharge areas 12–13, 15–19 and 21 (Table 3) for drinking water supply. The main reason of this is the expected increase in frequency and duration of low flow periods of the Rhine River and Meuse River, during which the rather steady water pollution load is far less diluted by base flow, storm water runoff or snow melt. The resulting interruption of artificial recharge and continued withdrawal of groundwater from the dunes may disturb the presence of rainwater lenses.

Conclusions

About 60 years of measurements with the 4 M-lysimeters near Castricum, each with a different, typical dune vegetation, yielded a very significant relation between the annual drainage quantity and annual rainfall, for each. Together with additional data from other studies, these relations formed the basis for a simple approximation of annual groundwater recharge in coastal dunes as function of annual precipitation and 11 vegetation types. The method should perform well along Atlantic sandy coasts with temperate climate.

Along the Dutch North Sea coast, freshwater lenses on salt groundwater were studied in the early 1900s, when they were still little disturbed by among others groundwater pumping. Evaluation of the very detailed and high quality data revealed that the Ghyben-Herzberg ratio of 40 is only

rarely encountered. On 21 coastal locations, the observed ratio was 18.6 on average, while ranging between 6 and 46. With an average salt water density of 1.020 kg/L, both below the lenses and along the Dutch coast, a ratio of 50 would be expected. The main reason for the much lower ratio consists of the presence of intercalated aquitards within the freshwater lens. This triggered the development of the here proposed, empirical correction factor for the height of the watertable, the depth to the fresh/salt interface and the lens formation time, as calculated with well known, closed-form analytical solutions from the literature.

A closed-form analytical solution is also presented for rainwater lenses that form where rain is falling and infiltrating on land next to infiltrating freshwater courses such as recharge basins or influent rivers.

All analytical solutions presented in this paper, can be easily applied to simulate or predict the effects of various environmental changes, such as sea level rise with coastal erosion, coastal progradation by sand nourishment, changes in groundwater recharge, an increase of hydraulic conductivity by a temperature increase, and changes in density of fresh or salt groundwater.

References

Arens SM, Geelen LHWT (2006) Dune landscape rejuvenation by intended destabilisation in the Amsterdam Water Supply Dunes. J Coast Res 22:1094–1107

Bakker TWM (1981) Dutch coastal dunes; geohydrology. Ph.D. thesis Wageningen University, Pudoc Wageningen (in Dutch), 189p

Bakker M (2006) Analytic solutions for interface flow in combined confined and semi-confined, coastal aquifers. Adv. Water Res 29(3):417–425

Bakker TWM, Jungerius PD, Klijn JA (eds) (1990) Dunes of the European coasts; geomorphology – hydrology - soils. Catena Suppl 18, Catena Verlag, Cremlingen-Destedt, Germany, 223p

Bear J (1979) Hydraulics of groundwater. McGraw-Hill Inc., 567p

Bear J & Todd DK (1960) The transition zone between fresh and salt water. Water Resor. Centre Contr. 29, Berkeley, Calif

Beijerinck MW, De Bruyn HE, Huffnagel P & Ribbius CPE (1909) Rapport der commissie van advies inzake de watervoorziening van de gemeente Delft, 141p

Berendsen HJA, Stouthamer E (2001) Palaeogeographic development of the Rhine-Meuse delta, The Netherlands. Koninklijke Van Gorcum, Assen, p. 268p

Beukeboom TJ (1976) The hydrology of the Frisian islands. Ph.D. Thesis Vrije Univ., Amsterdam, p. 121p

Bird E.C.F. 1981. World-wide trends in sandy shoreline changes during the past century. Géographie physique et Quaternaire, vol. 35, n°2, p. 241–244

Brown AC, McLachlan A (2002) Sandy shore ecosystems and the threats facing them: some predictions for the year 2025. Environ Conserv 29(1):62–77

Chesnaux R, Allen DM (2008) Groundwater travel times for unconfined island aquifers bounded by freshwater or seawater. Hydrogeol J 16:437–445

Curr RHF, Koh A, Edwards E, Williams AT, Daves P (2000) Assessing anthropogenic impact on Mediterranean sand dunes from aerial digital photography. J Coast Conserv 6:15–22

Defeo O, McLachlan A, Schoeman DS, Schlacher TA, Dugan J, Jones A, Lastra M, Scapini F (2009) Threats to sandy beach ecosystems: a review. Estuarine coastal and shelf. Science 81:1–12

Eisma D (1968) Composition, origin and distribution of Dutch coastal sands between Hoek van Holland and the island of Vlieland. Neth J Sea Res 4:123–267

Fetter CW (1972) Position of the saline water interface beneath oceanic islands. Water Resour Res 8:1307–1315

Geelen L, Salman A & Kuipers M [eds] (2015). Dynamic Dunes 2015; daring solutions for Natura 2000 challenges. Report of an international conference on rejuvenation of dynamic dunes and restoration of dune habitats, October 7–9, 2015, Zandvoort-Rockanje Netherlands. https://awd.waternet.nl/media/projecten/Life/PDF

Ghyben BW (1889) Nota in verband met de voorgenomen put-boring nabij Amsterdam (Notes on the results of the proposed well drilling in Amsterdam). Tijdschrift Koninklijk Instituut van Ingenieurs, The Hague, pp. 8–22

Greskowiak J, Roper T, Post VEA (2012) Closed-Form Approximations for Two-Dimensional Groundwater Age Patterns in a Fresh Water Lens. Ground water. doi:10.1111/j.1745-6584.2012.00996.x, 1-6

Grootjans AP, Esselink H, Van Diggelen R, Hartog P, Jager TD, Van Hees B & Oude MJ. (1997) Decline of rare calciphilous dune slack species in relation to decalcification and changes in local hydrological systems. In: The ecology and conservation of European dunes, Garcia NF, Crawford RMM & Barradas MCD [eds], Univ. Sevilla, 59–74

Grootjans AP, Dullo BS, Kooijman AM, Bekker RM & Aggenbach C. (2013) Restoration of dune vegetation in the Netherlands. Ch.15 in 'Restoration of coastal dunes', Martinez ML et al. [eds], Springer Series on Envir. Management, 235–254

Grunnet NM, Walstra DJR, Ruessink BG (2004) Process-based modelling of a shoreface nourishment. Coast Eng 51(7):581–607

Hansom JD (2001) Coastal sensitivity to environmental change: a view from the beach. Catena 42:291–305

Herrier J-L, Mees J, Salman A, Seys J, Van Nieuwenhuyse H & Dobbelaere I [eds] (2005) Proc. Dunes & Estuaries 2005, Internat. conf. on nature restoration, Koksijde, Belgium 19–23 September 2005, Flanders Marine Institute (VLIZ) Special Publication No. 19, 685p

Herzberg A (1901) Die Wasserversorgung einiger Nordseebäder. J. Gasbeleuchtung Wasserversorgung 44:815–819

Hillen R, Roelse P (1995) Dynamic preservation of the coastline in the Netherlands. J Coast Conserv 1:17–28

Houben G, Koeniger P, Sültenfuss J (2014) Freshwater lenses as archive of climate, groundwater recharge, and hydrochemical evolution: insights from depth-specific water isotope analysis and age determination on the island of Langeoog, Germany. Water Resour Res 50(10):8227–8239

Huisman L, Olsthoorn TN (1983) Artificial groundwater recharge. Pitman Adv. Publ, Program, 320p

Huizer S, Oude Essink GHP, Bierkens MFP (2016) Fresh groundwater resources in a large sand replenishment. Hydrol Earth Syst Sci Discuss. doi:10.5194/hess-2016-5

IPCC (2007) Climate Change 2007: The Physical Science Basis. Contribution of Working Group I to the Fourth Assessment Report of the Intergovernmental Panel on Climate Change [Solomon S, Qin D, Manning M, Chen Z, Marquis M, Averyt KB, Tignor M and Miller HL (eds.)]. Cambridge University Press, Cambridge, United Kingdom and New York, 996 pp

Jelgersma S, De Jong J, Zagwijn WH, Van Regteren Altena JF (1970) The coastal dunes of the western Netherlands; geology, vegetational history and archeology. Meded Rijks Geol Dienst NS 21:93–167

KNMI'14 (2015) Climate scenario's for the Netherlands. http://www.climatescenarios.nl/images/Climate_scenarios_EN_2015.pdf

Kooijman AM, Dopheide JCR, Sevink J, Takken I, Verstraten JM (1998) Nutrient limitations and their implications on the effects of atmospheric deposition in the coastal dunes; lime-poor and lime-rich sites in the Netherlands. J Ecol 86:511–526

Minderman G, Leeflang KWF (1968) The amount of drainage water and solutes from lysimeters planted with either oak, pine or natural dune vegetation or without any vegetation cover. Plant Soil 28:61–80

Olsthoorn TN (1982) Clogging of recharge wells. Kiwa Meded. 71 (in Dutch), Kiwa Meded. 72 (English summary)

Oude Essink GHP (1996) Impact of sea level rise on groundwater flow regimes; a sensitivity analysis for the Netherlands. PhD TU Delft, Delft Studies in Integrated Water Management No.7, 411p

Penman HL (1967) Evaporation from forests. In: Sopper WE & Lull HW [eds], 'Internat Symp. On Forest Hydrology', 373–380

Pluhowski EJ, Kantrowitz IH (1963) Influence of land-surface conditions on ground-water temperatures in southwestern Suffolk County, Long Island, New York. US Geol Survey Prof Paper 475-B:B186–B188

Röper T, Kröger F, Meyer H, Sültenfuss J, Massmann G (2012) Groundwater ages, recharge patterns and hydrochemical evolution of a barrier island freshwater lens (Spiekeroog, northern Germany. J Hydrol 454:173–183

Salman AHPM and Bonazountas M (Eds) (1996) Proceedings of the 4th EUCC conference in Marathon, Greece. Publ: EUCC, 2 Volumes, 1050p

Stoeckl L, Houben G (2012) Flow dynamics and age stratification of freshwater lenses: Experiments and modeling. J Hydrol 458–459:9–15

Stuyfzand PJ (1986) Water balances of and transit times within four lysimeters each with different vegetation, near Castricum. KIWA-report SWE-85.013, 53 p (in Dutch)

Stuyfzand PJ (1987) Effects of vegetation and air pollution on groundwater quality in calcareous coastal dunes near Castricum, the Netherlands: Lysimetric observations. Proc. Intern. Symp on Acidification and water pathways, Bolkesjo Norway 4–8 may 1987, Norw. Nat. Comm. for Hydrol. (ed), vol.2 , 115–125

Stuyfzand PJ (1993) Hydrochemistry and hydrology of the coastal dune area of the Western Netherlands. Ph.D Thesis Vrije Univ. Amsterdam, published by KIWA, ISBN 90-74741-01-0, http://dare.ubvu.vu.nl/handle/1871/12716, 366 p

Stuyfzand PJ (1998) Decalcification and acidification of coastal dune sands in the Netherlands. Water-Rock Interaction, Proc. 9th Intern. Symp. on WRI, Taupo New Zealand, Arehart GB & Hulston JR (eds), Balkema, 79–82

Stuyfzand PJ (2010) Multitracing of artificially recharged Rhine River water in the coastal dune aquifer system of the Western Netherlands. In 'Achieving groundwater supply, sustainability and reliability through Managed Aquifer Recharge', Proc ISMAR-7, Abu Dhabi, 9–13 Oct 2010, published 2012, p188–195, available on line via http://www.dina-mar.es

Stuyfzand PJ (2012) Hydrogeochemcal (HGC 2.1), for storage, management, control, correction and interpretation of water quality data in Excel (R) spread sheet. KWR Watercycle Research Institute, KWR-report BTO.2012.244(s),updated in Feb.2015, 82p

Stuyfzand PJ & Bruggeman GA (1994) Analytical approximations for fresh water lenses in coastal dunes. Proc. 13th Salt Water Intrusion Meeting, June 1994, Cagliari Italy, Barrocu G (ed), Univ. Cagliari, Fac. Engineering, 15–33

Stuyfzand PJ, Lüers F (1992) Hydrochemie en hydrologie van duinen en aangrenzende polders tussen Callantsoog en Petten. KIWA-rapport SWE-92(008):70p

Stuyfzand PJ & Rambags F (2011) Hydrology and hydrochemistry of the 4 lysimeters near Castricum; overview of results and feasibility of reanimation of the lysimeter station. KWR Rapport BTO 2011.020 (s), 111p (in Dutch)

Stuyfzand PJ & Stuurman RJ (1985) Experimenteel bewijs en modellering van een stationaire regenwaterlens op kunstmatig geinfiltreerd oppervlaktewater. H20 18, 408–415

Stuyfzand PJ, Lüers F, De Jonge HG (1993) Hydrochemie en hydrologie van duinen en aangrenzende polders tussen Katwijk en Kijkduin. KIWA-rapport SWE-93(001):165p

Stuyfzand PJ, Arens SM, Oost AP, Baggelaar PK (2012) Geochemical effects of sand nourishments in the Netherlands, along the coast from Ameland to Walcheren. Bosschap Report 2012/OBN167-DK, 150p (in Dutch)

Stuyfzand PJ, Amatirsat D, de Wagt Estrada I, van Bloemendal – Bland C, Oskam B, van Loon D, Everts H, Grootjans AP (2014) Zoet-zout gradiënten op 4 eilanden, in hydrologisch en hydrogeochemisch perspectief. KWR Rapport BTO 2014.221(s), 141p

Tollenaar P, Rijckborst H (1975) The effect of conifers on the chemistry and mass balance of two large lysi-meters in Castricum, The Netherlands. J Hydrol 24:77–87

Vacher HL (1988) Dupuit-Ghyben-Herzberg analysis of strip-island lenses. Geol Soc Am Bull 100:580–591

Van der Meulen F, Jungerius PD, Visser JH (1989) Perspectives in coastal dune management. SPB Academic Publ, The Hague, 333p

Van der Veer P (1977) Analytical solution for a two-fluid flow in a coastal aquifer involving a phreatic surface with precipitation. J Hydrol 35:271–278

Van Dijk HWJ (1989) Ecological impact of drinking water production in Dutch coastal dunes. In: Van der Meulen F, Jungerius PD, Visser JH (eds) Perspectives in coastal dune management. SPB Acad. Publ. B.V, The Hague, pp. 163–182

Van Oldenborgh J (1916) Mededelingen omtrent de uitkomsten van door het Rijksbureau voor Drink-watervoorziening ingestelde geohydrologische onderzoekingen in verschillende duingebieden. De Ingenieur 25, 458–467 en 26, 474–498

Verruijt A (1971) Steady dispersion across an interface in a porous medium. J Hydrol 14:337–347

Vidal R, Van Oord G (2010) Environmental impacts in beach nourishment: a comparison of options. Terra et Aqua 119:14–20

Zagwijn WH (1985) An outline of the Quarternary stratigraphy of The Netherlands. Geol Mijnb 64:17–24